EuroIntervention 2017;13:1242-1247 published online July 2017

Comparison of new-generation renal artery denervation systems: assessing lesion size and thermodynamics using a thermochromic liquid crystal phantom model

Sara I. Al Raisi[1,2], MB Bch, FRACP; Michael T. Barry[1,2], B.Sc; Pierre Qian[1,2], MBBS, FRACP; Abhishek Bhaskaran[2], MBBS, FRACP; Jim Pouliopoulos[1,2], PhD; Pramesh Kovoor[1,2]*, MBBS, PhD

1. Department of Cardiology, Westmead Hospital, Sydney, NSW, Australia; 2. University of Sydney, Sydney, NSW, Australia

KEYWORDS

- catheter ablation
- renal sympathetic denervation
- resistant hypertension

Abstract

Aims: The aim of this study was to evaluate and compare lesion dimensions and thermodynamics of the new-generation multi-electrode Symplicity Spyral and the new-generation multi-electrode EnligHTN renal artery denervation systems, using a thermochromic liquid crystal phantom model.

Methods and results: A previously described renal artery phantom model was used as a platform for radiofrequency ablation. A total of 32 radiofrequency ablations were performed using the multi-electrode Symplicity Spyral (n=16) and the new-generation EnligHTN systems (n=16). Both systems were used as clinically recommended by their respective manufacturer. Lesion borders were defined by the 51°C isotherm. Lesion size (depth and width) was measured and compared between the two systems. Mean lesion depth was 2.15±0.02 mm for the Symplicity Spyral and 2.32±0.02 mm for the new-generation EnligHTN (p-value <0.001). Mean lesion width was 3.64±0.08 mm and 3.59±0.05 mm (p-value=0.61) for the Symplicity Spyral and the new-generation EnligHTN, respectively.

Conclusions: The new-generation EnligHTN system produced lesions of greater depth compared to the Symplicity Spyral under the same experimental conditions. Lesion width was similar between both systems. Achieving greater lesion depth by use of the new-generation EnligHTN may result in better efficacy of renal artery denervation.

**Corresponding author: Department of Cardiology, PO Box 533, Westmead Hospital, Cnr of Hawkesbury and Darcy Road, Sydney, NSW, 2145, Australia. E-mail: pramesh.kovoor@sydney.edu.au*

SUBMITTED ON 03/04/2017 - REVISION RECEIVED ON 15/06/2017 - ACCEPTED ON 21/07/2017

DOI: 10.4244/EIJ-D-17-00278

Abbreviations

BP blood pressure
RAD renal artery denervation
RF radiofrequency
TLC thermochromic liquid crystal
SS Symplicity Spyral
NGE new-generation EnligHTN

Introduction

Following the encouraging results of the Symplicity HTN-1 and Symplicity HTN-2 trials, which demonstrated significant blood pressure (BP) reduction after renal artery denervation (RAD), endovascular radiofrequency (RF) ablation of the renal arteries was considered an acceptable treatment for drug refractory hypertension[1,2]. Later, the randomised controlled SYMPLICITY HTN-3 trial failed to show a significant difference in BP reduction between the RAD treatment arm and the sham control arm[3]. Nevertheless, the implication of renal sympathetic nerves in the pathogenesis of resistant hypertension has been well described and demonstrated in previous animal and human studies[4-8]. Several factors have been proposed that may have limited the denervation efficacy in SYMPLICITY HTN-3[9]. A better understanding of the basic mechanisms of denervation and factors affecting procedural success including patient selection, renal nerve anatomy and the biophysics of the various renal denervation systems through further preclinical studies is pivotal to achieving the desired results.

Previously, we developed a thermochromic liquid crystal (TLC) model and validated it *in vivo* for cardiac RF ablation[10]. Subsequently, we modified this model for renal denervation. In our previous study, we assessed and compared lesion size and thermodynamic properties of the single-electrode Symplicity (Flex) renal denervation system (Medtronic, Minneapolis, MN, USA) versus the first-generation multi-electrode EnligHTN system (St. Jude Medical, St. Paul, MN, USA) using the TLC renal artery phantom model[11]. Recently, in the new-generation systems, several modifications have been applied to both the EnligHTN and Symplicity renal denervation systems in order to overcome some of the technical procedural challenges, and to reduce overall procedural duration, either of which could ultimately impact on ablation efficacy. Therefore, in this study we aimed to evaluate and assess the performance of the new-generation Symplicity Spyral (SS) and the new-generation EnligHTN (NGE) renal denervation systems using the previously described renal artery phantom model. **Table 1** summarises the differences between the old and the new Symplicity and EnligHTN systems.

Methods

Radiofrequency ablations for both the SS and NGE systems were performed in the renal artery phantom model using clinically recommended ablation settings **(Table 1)**. Temporal changes in lesion dimensions (depth and width) for the two systems were measured and compared.

THERMOCHROMIC LIQUID CRYSTAL PHANTOM RENAL ARTERY MODEL

The renal artery phantom model was prepared as previously described[11]. In summary, a mixture of saline and an agar substitute powder (Phytagel™; Sigma-Aldrich [now Merck], St. Louis, MO, USA) was heated to 90°C in a preformed cast encompassing a 5 mm diameter cylindrical former. Once cooled, the former was removed to create a transparent block of gel with a 5 mm diameter lumen to simulate the renal artery. A TLC film that has temperature sensitivity between 50-78°C (Hallcrest LCR, Connah's Quay, United Kingdom) was embedded within the gel prior to solidification. The gel block was placed in a tank, which pumped saline around the gel and into the phantom renal artery lumen at a rate of 500 ml/min and a temperature of 37°C.

RADIOFREQUENCY ABLATION

The ablation catheter for the system was introduced into the phantom renal artery under direct visualisation. The Spyral catheter was advanced into the phantom lumen over a (0.014-inch) guidewire as clinically recommended. Once within the lumen of the phantom renal artery, the guidewire was pulled back to allow spiral configuration of the catheter. In the case of the EnligHTN catheter, a small diameter basket size (recommended for vessel diameters between 4 and 6 mm) was used and the catheter was deployed on a single instance per gel to limit abrasion of the gel surface. At least one electrode was positioned in plane with the TLC sheet. Only the electrode in contact with the TLC sheet was activated for each RF ablation (one electrode per run). All ablations were performed with

Table 1. Summary of the technical specifications and a comparison between the new and old Symplicity and EnligHTN renal denervation systems.

System	Old systems		New systems	
	Symplicity (Flex)	EnligHTN old generation	Symplicity (Spyral)	EnligHTN new generation
Generator	Symplicity G2	1st generation	Symplicity G3	2nd generation
Number of electrodes	1	4	4	4
Ablation duration (sec)	120	90	60	60
Maximum power per electrode (W)	8	6	6.5	8
Electrode surface area (mm^2)*	6.39	3.7	5.9	3.7

* Measured in-house.

a flow rate of 500 ml/min through the phantom renal artery, and an ablation duration of 60 sec. The gel was allowed to cool down for five minutes between RF ablations and the catheter was moved to a new position after four runs of ablation.

LESION MEASUREMENTS AND ANALYSIS

A digital camera (Canon EOS 5D Mark II; Canon Inc., Tokyo, Japan) with a light source (Canon Speedlite 580EX; Canon) was placed in front of the phantom model to capture images at different ablation time points (at baseline, 20 sec, 30 sec, 40 sec, 50 sec and 60 sec). Heating of the gel at the TLC surface produced a colour gradient on the TLC sheet **(Figure 1A)**, which was utilised to calculate the isotherms following thermochromic calibration using in-house developed software **(Figure 1B)**. The 51°C isotherm was used as an arbitrary measure to define lesion borders, as irreversible neural tissue injury occurs at temperatures greater than 45-50°C[12,13]. Lesion depth (*d*) was measured as the length of a line between the electrode/gel interface and the 51°C isotherm perpendicular to the electrode tip. Lesion width (*w*) was defined as the maximum width of the 51°C isotherm perpendicular to *d* **(Figure 1B)**.

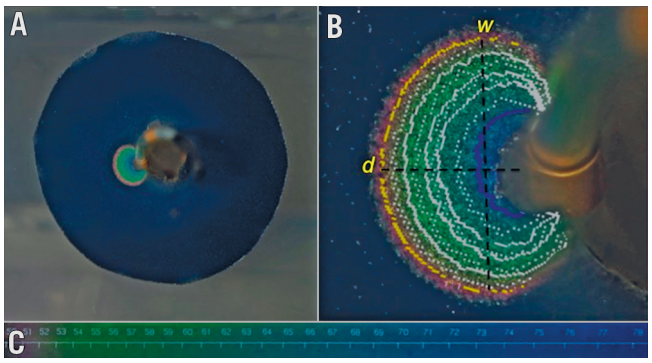

Figure 1. *Image taken during radiofrequency ablation on the phantom renal artery model at 60 sec using the Symplicity Spyral system in this case. A) Colour gradient on the TLC sheet during RF ablation. B) Lesion post analysis with superimposed isotherms. Yellow line highlights the 51°C isotherm. C) Colour gradient with the corresponding temperature in °C. d: lesion depth; w: lesion width; TLC: thermochromic liquid crystal*

STATISTICAL ANALYSIS

Based on previous work in the same phantom model, RF ablation in replicates of three per catheter were required to detect a significant difference in lesion size, with a power of 95% and α=0.05 (two-tailed), for each parameter tested[11]. Mean lesion depth and width for each system were compared using an unpaired two-tailed Student's t-test. Data were expressed as mean±standard deviation. The relationship between lesion growth (depth and width) and time was assessed using Spearman's correlation. Values of p<0.05 were considered significant. Data analysis was performed with GraphPad Prism software 6.0 (GraphPad Software Inc., La Jolla, CA, USA) and SPSS, Version 24 (IBM Corp., Armonk, NY, USA).

Results

A total of 32 RF ablations (16 ablations per system) were performed on the phantom renal artery model. All ablations were carried out under similar phantom conditions whereby parameters, including phantom vessel diameter, flow rate and gel temperature, were adjusted to within normal physiological ranges of 5 mm, 500 ml/min and 37°C, respectively. **Table 2** summarises the ablation parameters for both systems.

Table 2. Ablation parameters for Symplicity Spyral and new-generation EnligHTN systems.

System	Symplicity Spyral	New-generation EnligHTN	*p*-value
Ablation number	16	16	–
Mean power (V)	6.5±0.00 (maximum power)	5.3±0.07 (average power)	–
Mean baseline impedance (Ω)	174.3±0.88	199.1±0.88	<0.001
Mean electrode tip temperature (°C)	45.56±0.66 (maximum temperature)	52.50±0.98 (average temperature)	–
Ablation duration (sec)	60	60	–

LESION SIZE AND GROWTH

Thirty-one RF ablation lesions (16 for SS and 15 for NGE) were analysed at 60 sec to determine final lesion size. A single data point for the NGE group was unavailable due to photographic aberration. Immediately prior to termination of RF ablation (60 sec), mean lesion depth for SS was 2.15±0.02 mm versus 2.32±0.02 mm for NGE (p-value <0.001) **(Figure 2A)**. Mean lesion width was 3.64±0.08 mm and 3.59±0.04 mm (p-value=0.61) for SS and NGE, respectively **(Figure 2B)**.

In addition, temporal analysis of lesion dimensions was performed to demonstrate the thermodynamics of each ablation system **(Figure 3)**. A Spearman correlation test demonstrated a strong positive correlation between the duration of RF ablation and lesion size (depth and width), which was statistically significant for both systems. The correlation coefficient (r_s) for ablation duration versus lesion depth was 0.91 (p<0.001) for SS and 0.86 (p<0.001) for NGE. The correlation coefficient (r_s) for ablation duration versus lesion width was 0.606 (p<0.001) and 0.726 (p<0.001) for SS and NGE, respectively.

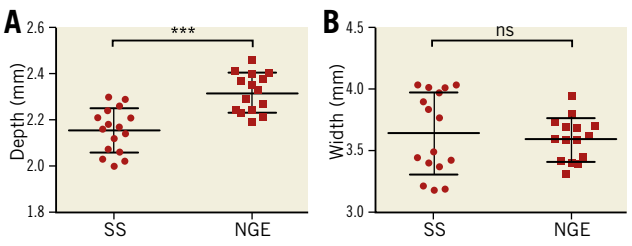

Figure 2. *Scatter plots comparing lesion depth and width for the Symplicity Spyral and new-generation EnligHTN sytems at end of radiofrequency ablation (60 sec). A) Lesion depth. B) Lesion width. NGE: new-generation EnligHTN; SS: Symplicity Spyral*

Graphs of lesion depth and width over time **(Figure 3)** suggest that prolonging the ablation duration could potentially increase lesion size, as a plateau phase has not been reached. Nonetheless, analysis of lesion size at different ablation time points demonstrated that about 70-80% of lesion growth occurred within the first 20 sec of RF delivery with a lesion growth rate of 0.076 mm/sec for depth and 0.147 mm/sec for width with SS, and 0.094 mm/sec for depth and 0.124 mm/sec for width with NGE during the initial 20 sec ablation phase. Lesion growth rate slows down thereafter to 0.012 mm/sec for depth and 0.01 mm/sec for width with SS and 0.009 mm/sec for depth and 0.008 mm/sec for width with NGE in the last 20 sec of RF ablation. Thus, increasing ablation time beyond 60 sec may result in only a small increase in lesion size. **Table 3** summarises lesion dimensions at 20, 40 and 60 seconds of RF ablation and the percentage of lesion growth (depth and width) at each time point.

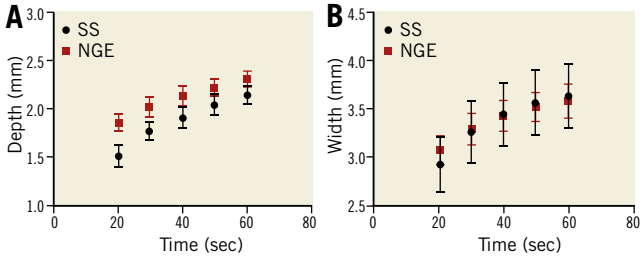

Figure 3. *Graph demonstrating the relationship between radiofrequency ablation duration and lesion growth for the Symplicity Spyral and new-generation EnligHTN systems. A) Lesion depth versus time. B) Lesion width versus time. NGE: new-generation EnligHTN; SS: Symplicity Spyral*

Discussion

Using the TLC renal artery phantom model, the NGE renal denervation system achieved greater lesion depth compared to the multi-electrode SS system. However, there was no difference in lesion width between the two systems. RF ablation with both systems was performed under consistent experimental settings (i.e., consistent gel impedance, gel temperature, vessel diameter and flow rate) and optimal electrode/gel contact as confirmed by direct visualisation. Our phantom model allows direct comparison due to the ability to control variables, which is difficult to achieve clinically.

In our previous study, we compared the lesion dimensions and thermal properties of the single-electrode Symplicity Flex versus the first-generation multi-electrode EnligHTN renal artery denervation system, utilising the same renal artery phantom model[11]. The present study is the first to compare the new-generation multi-electrode Spyral system to the new-generation EnligHTN system using the TLC/gel phantom model. In RF ablation, only about 1 mm of tissue adjacent to the electrode (area of resistive heating) is heated directly. Deeper tissue is heated by conduction of thermal energy from the resistive heating zone[14].

Therefore, increased heating at the electrode tissue interface leads to more heat being conducted through the tissue and subsequently larger lesions. This is affected by several factors including ablation power, electrode size, electrode area in contact with tissue, contact force, convective cooling and ablation duration[14,15]. Whilst the SS electrode surface area is larger compared to the NGE **(Table 1)**, lesions produced by the SS were comparatively smaller in depth. It has been demonstrated that increased electrode surface area results in larger lesions. Nonetheless, electrodes with a larger surface area usually require higher power delivery to maintain the same current density at the electrode tissue interface[16-19]. The maximum power generated by the SS and NGE is 6.5 W and 8 W, respectively. Conversely, a larger electrode area leads to more heat loss in the blood pool by convection and, therefore, reduces heating efficiency. Power lost in the blood pool is even greater when electrode-tissue contact is reduced[15]. It is possible that the greater contact force produced by the EnligHTN catheter upon deployment results in more optimal and stable gel contact, and therefore deeper lesions. It is important to note that for all ablations careful placement of the electrode tip against the TLC/gel surface was consistent and confirmed. Haines demonstrated in an *in vitro* model that greater contact pressure produced deeper lesions as long as electrode-tissue contact was maintained and electrode-tissue temperature kept constant by adjusting power. In his study, lesion width showed no significant difference with increased contact force[20]. Consistent with this finding, we found no difference in width between the two systems. Although not directly measured, it is likely to be the design of the EnligHTN catheter that has the advantage of producing more consistent contact force. This could also explain the lower electrode tip temperature achieved by the SS **(Table 2)**.

Of note, when the old-generation systems were used in the same model, the lesions produced were deeper (3.8 mm and 3.4 mm for Symplicity and EnligHTN, respectively)[11]. A recent animal study also suggested a thermal injury depth of 3.9 mm when the Symplicity

Table 3. Lesion size and the percentage of growth at 20, 40 and 60 sec during radiofrequency ablation for Symplicity Spyral and new-generation EnligHTN.

Ablation time (sec)	Depth (mm)		*p*-value	Width (mm)		*p*-value	% Depth:width of maximum	
	SS	NGE		SS	NGE		SS	NGE
20	1.52±0.03	1.87±0.02	<0.001	2.93±0.07	3.08±0.04	0.10	70.7:80.7	80.6:85.8
40	1.92±0.03	2.14±0.03	<0.001	3.45±0.08	3.44±0.04	0.86	89.3:95.0	92.2:95.8
60	2.15±0.02	2.32±0.02	<0.001	3.63±0.08	3.59±0.05	0.61	100:100	100:100

NGE: new-generation EnligHTN; SS: Symplicity Spyral

Flex was used[21]. Although the old- and the new-generation systems were not directly compared, the conditions of the phantom model were consistent between time points, suggesting a difference in performance between the old- and the new-generation systems. In the case of the SS, a 50% reduction in ablation duration with lower power output compared to the old Symplicity system may have resulted in reduced net current density at the electrode-tissue interface despite the marginally smaller electrode surface area of this system. In addition, increased contact force at the tip of the Symplicity Flex catheter due to the ability to deflect the tip vector towards the gel interface could have produced a degree of contact force that minimised heat loss. For the NGE, smaller depth compared to the old EnligHTN system is probably partially due to shorter ablation duration.

Lesion size is one of several important elements for achieving clinical efficacy in RAD. Deeper lesions may translate into more effective denervation, as more nerve bundles could be targeted. Clinically, successful denervation is important in order to achieve a significant BP reduction after RAD. Evidence from post-mortem and animal studies has demonstrated that about 50% of renal nerves proximal to the bifurcation are located at a depth of greater than 2.44 mm[22,23]. Therefore, given the findings of the present study, ablation using the new-generation systems may potentially result in denervation of <50% of renal nerves at those sites, thus limiting the efficacy of the procedure. When assessing nerves at different vessel segments, it has been shown that most of the nerve bundles are located within the proximal and middle segments of the renal arteries. However, they are found at a greater depth in the proximal segment compared to the distal segment of the vessel (3.4 mm proximally versus 2.6 mm distally), which renders the proximal nerve bundles more difficult to ablate endovascularly using the currently available denervation systems[22]. In distal segments (before the bifurcation), the 50th percentile of nerves was found to be at 1.81 mm from the lumen; 79% of nerves found distal to the bifurcation are located within 2 mm from the lumen[22]. The limited depth of heating and the current knowledge of renal nerve distribution highlight the importance of distal segment ablation. This was demonstrated in a porcine model study by Mahfoud et al, where the addition of ablation distal to the bifurcation using the SS resulted in more effective denervation as measured by a reduction in cortical norepinephrine content and axonal density compared to main vessel ablation only[24].

While the focus now has been directed towards more distal denervation (distal segment and distal to the bifurcation), improving ablation systems to reach deeper targets may also be beneficial, if this could be attained safely. Initial experimental studies using alternative energy modalities, including microwave ablation and chemical denervation, reported on lesion depth of 5-8 mm[21,25]. However, until additional research is conducted to evaluate the efficacy and safety of such modalities further, their use remains experimental.

Study limitations

Ablation conditions on the phantom renal artery model used in this study do not represent the complete spectrum of physiological conditions and acute response to RF ablation during renal denervation. In addition, the design of the current model allows assessment of heating pattern on a single plane only. Therefore, we were unable to assess heating of all four electrodes simultaneously, which may have an effect on heating pattern. However, the ability to control different variables and standardise the model allows us to compare the two systems under identical settings. Moreover, the effect of altering different parameters on lesion size could be assessed using this model in future studies. Lastly, we have chosen the 51°C isotherm to define lesion dimension. However, if nerve injury occurs at temperatures above or below this threshold, the actual depth of thermal injury would be underestimated or overestimated. Nonetheless, for the application of RF ablation in neurosurgery it has been generally accepted that neural tissue destruction occurs at temperature ≥45-50°C (lethal isotherm) and temperatures between 42-45°C showed reversible neural damage[13,26].

Conclusions

Increased lesion depth was achieved using the NGE renal denervation system compared to the SS system for ablation on the TLC phantom model, with no difference in lesion width. Whilst the difference in depth is small, it may have an impact on denervation efficacy.

Impact on daily practice

The relationship between the renal nerves as a target for radiofrequency ablation and ablation depth is one of several factors affecting denervation success. Information on different devices and technologies available with regard to their thermal properties and biophysics can guide clinicians as well as help us to understand the limitations of currently available systems and possible areas for improvement.

Funding

Symplicity Spyral and EnligHTN catheters were donated by Medtronic and St. Jude Medical. S. Al Raisi is supported by a Research Training Program Stipend scholarship (SC1999). P. Qian is supported by a National Health and Medical Research Council (NHMRC) and National Heart Foundation of Australia (NHF) co-funded postgraduate scholarship (NHMRC Scholarship No. 1114408, NHF Scholarship No. 101107).

Conflict of interest statement

P. Qian and M. Barry are inventors of a microwave catheter for renal artery denervation. The intellectual property is owned by the University of Sydney and Westmead Hospital, Australian Patent AU2015902225, issued 12-06-2015. The other authors have no conflicts of interest to declare.

References

1. Krum H, Schlaich M, Whitbourn R, Sobotka PA, Sadowski J, Bartus K, Kapelak B, Walton A, Sievert H, Thambar S, Abraham WT,

Esler M. Catheter-based renal sympathetic denervation for resistant hypertension: a multicentre safety and proof-of-principle cohort study. *Lancet.* 2009;373:1275-81.

2. Symplicity HTN-2 Investigators, Esler M, Krum H, Sobotka PA, Schlaich MP, Schmieder RE, Böhm M. Renal sympathetic denervation in patients with treatment-resistant hypertension (The Symplicity HTN-2 Trial): a randomised controlled trial. *Lancet.* 2010;376:1903-9.

3. Bhatt DL, Kandzari DE, O'Neill WW, D'Agostino R, Flack JM, Katzen BT, Leon MB, Liu M, Mauri L, Negoita M, Cohen SA, Oparil S, Rocha-Singh K, Townsend RR, Bakris GL; SYMPLICITY HTN-3 Investigators. A controlled trial of renal denervation for resistant hypertension. *N Engl J Med.* 2014;370:1393-401.

4. DiBona GF. Physiology in perspective: The Wisdom of the Body. Neural control of the kidney. *Am J Physiol Regul Integr Comp Physiol.* 2005;289:R633-41.

5. Esler M, Jennings G, Lambert G. Noradrenaline release and the pathophysiology of primary human hypertension. *Am J Hypertens.* 1989;2:140S-146S.

6. Campese VM, Kogosov E, Koss M. Renal afferent denervation prevents the progression of renal disease in the renal ablation model of chronic renal failure in the rat. *Am J Kidney Dis.* 1995;26:861-5.

7. Katholi RE, Winternitz SR, Oparil S. Decrease in peripheral sympathetic nervous system activity following renal denervation or unclipping in the one-kidney one-clip Goldblatt hypertensive rat. *J Clin Invest.* 1982;69:55-62.

8. Esler M, Jennings G, Korner P, Blombery P, Sacharias N, Leonard P. Measurement of total and organ-specific norepinephrine kinetics in humans. *Am J Physiol.* 1984;247:E21-8.

9. Kandzari DE, Bhatt DL, Brar S, Devireddy CM, Esler M, Fahy M, Flack JM, Katzen BT, Lea J, Lee DP, Leon MB, Ma A, Massaro J, Mauri L, Oparil S, O'Neill WW, Patel MR, Rocha-Singh K, Sobotka PA, Svetkey L, Townsend RR, Bakris GL. Predictors of blood pressure response in the SYMPLICITY HTN-3 trial. *Eur Heart J.* 2015;36:219-27.

10. Chik WW, Barry MA, Thavapalachandran S, Midekin C, Pouliopoulos J, Lim TW, Sivagangabalan G, Thomas SP, Ross DL, McEwan AL, Kovoor P, Thiagalingam A. High spatial resolution thermal mapping of radiofrequency ablation lesions using a novel thermochromic liquid crystal myocardial phantom. *J Cardiovasc Electrophysiol.* 2013;24:1278-86.

11. Al Raisi SI, Pouliopoulos J, Barry MT, Swinnen J, Thiagalingam A, Thomas SP, Sivagangabalan G, Chow C, Chong J, Kizana E, Kovoor P. Evaluation of lesion and thermodynamic characteristics of Symplicity and EnligHTN renal denervation systems in a phantom renal artery model. *EuroIntervention.* 2014;10:277-84.

12. Cosman ER Jr, Cosman ER Sr. Electric and thermal field effects in tissue around radiofrequency electrodes. *Pain Med.* 2005;6:405-24.

13. Cosman ER Jr, Cosman ER Sr. Radiofrequency Lesions, in: Lozano AM, Gildenberg PL, Tasker RR, editors. Textbook of stereotactic and functional neurosurgery. 2nd ed. Berlin, Heidelberg, Germany: Springer Science & Business Media; 2009. p.1359-80.

14. Nath S, DiMarco JP, Haines DE. Basic aspects of radiofrequency catheter ablation. *J Cardiovasc Electrophysiol.* 1994;5:863-76.

15. Wittkampf FH, Nakagawa H. RF catheter ablation: Lessons on lesions. *Pacing Clin Electrophysiol.* 2006;29:1285-97.

16. Haines DE, Watson DD, Verow AF. Electrode radius predicts lesion radius during radiofrequency energy heating. Validation of a proposed thermodynamic model. *Circ Res.* 1990;67:124-9.

17. Otomo K, Yamanashi WS, Tondo C, Antz M, Bussey J, Pitha JV, Arruda M, Nakagawa H, Wittkampe F, Lazzara R, Jackman W. Why a large tip electrode makes a deeper radiofrequency lesion: effects of increase in electrode cooling and electrode-tissue interface area. *J Cardiovasc Electrophysiol.* 1998;9:47-54.

18. Kovoor P, Daly M, Campbell C, Dewsnap B, Eipper V, Uther J, Ross D. Intramural radiofrequency ablation: effects of electrode temperature and length. *Pacing Clin Electrophysiol.* 2004;27:719-25.

19. Langberg JJ, Gallagher M, Strickberger SA, Amirana O. Temperature-guided radiofrequency catheter ablation with very large distal electrodes. *Circulation.* 1993;88:245-9.

20. Haines DE. Determinants of Lesion Size During Radiofrequency Catheter Ablation: The Role of Electrode-Tissue Contact Pressure and Duration of Energy Delivery. *J Cardiovasc Electrophysiol.* 1991;2:509-15.

21. Bertog S, Fischel TA, Vega F, Ghazarossian V, Pathak A, Vaskelyte L, Kent D, Sievert H, Ladich E, Yahagi K, Virmani R. Randomised, blinded and controlled comparative study of chemical and radiofrequency-based renal denervation in a porcine model. *EuroIntervention.* 2017;12:e1898-906.

22. Sakakura K, Ladich E, Cheng Q, Otsuka F, Yahagi K, Fowler DR, Kolodgie FD, Virmani R, Joner M. Anatomic assessment of sympathetic peri-arterial renal nerves in man. *J Am Coll Cardiol.* 2014;64:635-43.

23. Tellez A, Rousselle S, Palmieri T, Rate WR 4th, Wicks J, Degrange A, Hyon CM, Gongora CA, Hart R, Grundy W, Kaluza GL, Granada JF. Renal artery nerve distribution and density in the porcine model: biologic implications for the development of radiofrequency ablation therapies. *Transl Res.* 2013;162:381-9.

24. Mahfoud F, Tunev S, Ewen S, Cremers B, Ruwart J, Schulz-Jander D, Linz D, Davies J, Kandzari DE, Whitbourn R, Böhm M, Melder RJ. Impact of Lesion Placement on Efficacy and Safety of Catheter-Based Radiofrequency Renal Denervation. *J Am Coll Cardiol.* 2015;66:1766-75.

25. Qian PC, Barry MA, Al Raisi S, Kovoor P, Pouliopoulos J, Nalliah CJ, Bhaskaran A, Chik W, Kurup R, James V, Verikatt W, McEwan A, Thiagalingam A, Thomas SP. Transcatheter non-contact microwave ablation may enable circumferential renal artery denervation while sparing the vessel intima and media. *EuroIntervention.* 2017;12:e1907-15.

26. Cosman ER Jr, Dolensky JR, Hoffman RA. Factors that affect radiofrequency heat lesion size. *Pain Med.* 2014;15:2020-36.